

The cotton MAPK kinase GhMPK20 negatively regulates resistance to *Fusarium oxysporum* by mediating the MKK4–MPK20–WRKY40 cascade

CHEN WANG¹, XIAOWEN HE², YUZHEN LI¹, LIJUN WANG¹, XULEI GUO¹ AND XINGQI GUO¹, *

¹State Key Laboratory of Crop Biology, College of Life Sciences, Shandong Agricultural University, Taian, Shandong 271018, China

²State Key Laboratory of Crop Biology, Shandong Agricultural University, Taian, Shandong 271018, China

SUMMARY

Fusarium wilt is one of the most serious diseases affecting cotton. However, the pathogenesis and mechanism by which *Fusarium oxysporum* overcomes plant defence responses are unclear. Here, a new group D mitogen-activated protein kinase (MAPK) gene, *GhMPK20*, was identified and functionally analysed in cotton. *GhMPK20* expression was significantly induced by *F. oxysporum*. Virus-induced gene silencing (VIGS) of *GhMPK20* in cotton increased the tolerance to *F. oxysporum*, whereas ectopic *GhMPK20* overexpression in *Nicotiana benthamiana* reduced *F. oxysporum* resistance via disruption of the salicylic acid (SA)-mediated defence pathway. More importantly, an *F. oxysporum*-induced MAPK cascade pathway composed of *GhMCK4*, *GhMPK20* and *GhWRKY40* was identified. VIGS of *GhMCK4* and *GhWRKY40* also enhanced *F. oxysporum* resistance in cotton, and the function of GhMCK4–GhMPK20 was shown to be essential for *F. oxysporum*-induced *GhWRKY40* expression. Together, our results indicate that the GhMCK4–GhMPK20–GhWRKY40 cascade in cotton plays an important role in the pathogenesis of *F. oxysporum*. This research broadens our knowledge of the negative role of the MAPK cascade in disease resistance in cotton and provides an important scientific basis for the formulation of *Fusarium* wilt prevention strategies.

Keywords: cotton, *Fusarium oxysporum*, *Gossypium hirsutum*, MAPK cascade, negative regulation.

INTRODUCTION

Plants have been exposed to many pathogens and have evolved multiple mechanisms of innate immunity (Jones and Takemoto, 2004). In general, the plant innate immunity system has two main branches: pathogen-associated molecular pattern (PAMP)-triggered immunity (PTI) and effector-triggered immunity (ETI) (Jones and Dangl, 2006; Medzhitov and Janeway, 1997). Successful pathogens can invade and colonize plants by the suppression of host

immunity systems. Bacterial pathogens can inhibit the defence signalling pathway by the secretion of effector molecules (Schechter *et al.*, 2006). Similarly, fungi secrete a wide diversity of effectors into host cells to manipulate plant immunity (Yu X *et al.*, 2012).

Plant immunity systems are tightly controlled by many phytohormones and a series of complex signal transduction processes. Salicylic acid (SA) and jasmonic acid (JA) are the most important hormones for plant immunity systems (Thaler *et al.*, 2012). SA is an essential signalling molecule that induces systemic acquired resistance (SAR) and is primarily affected by responses to biotrophic pathogens (Glazebrook, 2005). The JA-mediated pathway is primarily induced by resistance to herbivores and necrotrophic pathogens (Glazebrook, 2005). The SA pathway is typically prioritized over the JA pathway, and signalling crosstalk between SA and JA commonly manifests as reciprocal antagonism and may be adaptive (Thaler *et al.*, 2012). Amongst the intricate signalling networks, mitogen-activated protein kinase (MAPK) cascades are the major modules that identify and amplify external signals into intracellular components (Meng and Zhang, 2013; Rodriguez *et al.*, 2010). MAPK cascade activation is one of the cellular responses induced following PAMP recognition in plants (Asai *et al.*, 2002). Canonical MAPK cascades include three tiers of reversibly phosphorylated kinases: MAPK kinase (MAPKK) kinases (MAPKKKs), MAPKKs and MAPKs (Rodriguez *et al.*, 2010). Previous studies have reported that many pathogens disrupt plant immunity by perturbing the plant MAPK pathways. *AtMPK4* is a widely studied MAPK gene, and the activation of MAPK4 by flg22 negatively regulates the innate immune response in plants (Gao *et al.*, 2008). Overexpression of a *Pseudomonas syringae* effector, *HopA11*, inhibits MPK3 and MPK6 activation in response to flg22 in *Arabidopsis* (Zhang *et al.*, 2007). In addition, HopF2, another *P. syringae* effector, blocks the kinase activity of MKK5 via its ADP-ribosyltransferase activity (Feng and Zhou, 2012). In addition to bacterial pathogens, fungal pathogens attack plants by the disruption of plant MAPK cascades. As a model fungus, the mechanism of *Phytophthora infestans* infection has been widely studied. *Phytophthora infestans* is a member of a genus of pathogens destructive to members of the nightshade family. *Phytophthora infestans* secretes effectors to manipulate host innate immunity (Yang *et al.*, 2017). For example, Avh238 and Avh241

*Correspondence: Email: xqguo@sdau.edu.cn

are the RxLR effectors of *P. infestans* that cause cell death in various plant species (Yang *et al.*, 2017; Yu X *et al.*, 2012). Recent studies have reported that Avh238- and Avh241-triggered cell death is required for the mitogen-activated protein kinase kinase 2 (MEK2)–wound-induced protein kinase (WIPK) cascade in *Nicotiana benthamiana* (Yang *et al.*, 2017; Yu X *et al.*, 2012). However, the infection mechanisms of other fungi and the mechanisms by which fungi disrupt plant MAPK cascades are unclear.

MAPK cascades affect plant innate immune responses by interacting with their substrates, and WRKY transcription factors (TFs) are essential MAPK substrates (Zhang T *et al.*, 2016). WRKY TFs have been shown to bind W-box [TTGACC(T)] in the promoter regions of target genes (Rushton *et al.*, 2010), and many studies have reported that WRKY TFs are involved in the regulation of plant defence responses to pathogens (Rushton *et al.*, 2010). In *Arabidopsis*, *AtWRKY33* has been shown to regulate both SA- and JA-mediated defence pathways (Birkenbihl *et al.*, 2012), and *OsWRKY30* overexpression has been shown to increase resistance to rice fungal pathogens by positively regulating the JA-mediated pathway in rice (Peng *et al.*, 2012). However, little is known about the function of WRKY TFs with regard to the defence response in non-model plants, and potential mechanisms underlying the negative regulation of WRKY TFs on the plant defence response remain ambiguous.

Cotton (*Gossypium hirsutum*) is one of the most important fibre- and oil-producing commercial crops (Sunilkumar *et al.*, 2006). Fusarium wilt and Verticillium wilt are the fungal diseases that are the greatest threat to cotton. *Fusarium oxysporum* f. sp. *vasinfectum* is the main cause of Fusarium wilt disease and is present in almost all cotton-growing regions worldwide (Gaspar *et al.*, 2014). Fusarium wilt is a vascular disease that causes the vascular tissue to turn brown and results in substantial crop losses. *Fusarium oxysporum* infects the roots and then enters the vascular tissue, where it secretes many virulence determinants, such as small peptides or phytotoxins (Pietro *et al.*, 2003). Many studies have reported that *F. oxysporum*, similar to other fungal pathogens, has evolved multiple strategies to counter plant immunity systems (Morrissey and Osbourn, 1999). The *F. oxysporum* *SNF1* (*FoSNF1*) gene may encode a cell wall-degrading enzyme. Mutations in *FoSNF1* reduce the virulence of *F. oxysporum* by repressing the production of cell wall-degrading enzymes (Ospina-Giraldo *et al.*, 2003). In addition, the Six1 protein is secreted by *F. oxysporum* during xylem colonization and is required for full virulence of *F. oxysporum* f. sp. *lycopersici* in susceptible tomato lines (Rep *et al.*, 2005). However, few studies have examined the pathogenesis of *F. oxysporum* disruption of defence responses in cotton.

Upland cotton is an allotetraploid that most probably arose from interspecific hybridization (Page *et al.*, 2013). Previously, 56 MAPKs and 102 WRKYs have been confirmed in upland cotton by genome-wide analysis (Dou *et al.*, 2014; Zhang X *et al.*, 2016). Some MAPKs, such as *GhMPK7* (Shi *et al.*, 2010), *GhMPK11*

(Wang F *et al.*, 2016) and *GhMPK16* (Shi *et al.*, 2011), and WRKYs, such as *GhWRKY15* (Yu F *et al.*, 2012), *GhWRKY27a* (Yan *et al.*, 2015) and *GhWRKY40* (Wang *et al.*, 2014), have been shown to affect plant defence responses.

In this study, a new cotton group D MAPK gene, *GhMPK20*, was identified and characterized. Silencing of *GhMPK20* in cotton enhanced the tolerance to *F. oxysporum*, and ectopic *GhMPK20* overexpression in *N. benthamiana* reduced the resistance to *F. oxysporum*. More importantly, results from a series of genetic and biochemical analyses indicated that *GhMPK20* plays an important role in the pathogenic process of *F. oxysporum* in cotton via the MKK4–MPK20–WRKY40 pathway. Together, these results broaden our knowledge regarding the biological roles of the MAPK cascade in disease resistance, and significantly improve our understanding of the pathogenesis of *F. oxysporum*.

RESULTS

Characterization and subcellular localization of *GhMPK20*

Many recent studies have reported that MAPKs play important roles in plant disease resistance in *Arabidopsis thaliana* (MAPK Group, 2002). To identify new *F. oxysporum*-induced MAPK genes in cotton, we detected the expression levels of MAPK genes in cotton after *F. oxysporum* infection, and expression analyses were performed in the cotton cotyledon. One MAPK gene, designated *GhMPK20*, was chosen for detailed characterization because it was significantly induced by *F. oxysporum* (more than eight-fold) (Fig. S1A, see Supporting Information).

The full-length *GhMPK20* cDNA (GenBank accession number: HQ828072) is 2085 bp, with a 71-bp 5'-untranslated region (UTR), 193-bp 3'-UTR and 1821-bp open reading fragment (ORF), encoding a 606-amino-acid peptide with a predicted molecular weight of 69.16 kDa and an isoelectric point of 9.22. Phylogenetic analysis showed that *GhMPK20* can be clustered into the group D MAPK family (Fig. S2, see Supporting Information). Multiple sequence alignments demonstrated that *GhMPK20* shares high homology with other group D members, such as *A. thaliana* *AtMPK20* (73.49%), *G. hirsutum* *GhMPK16* (60.79%) and *Oryza sativa* *OsMPK20* (72.98%) (Fig. 1A). *GhMPK20* also exhibits significant family similarity, with 11 conserved subdomains, a phosphorylation motif (TDY motif) in an activation loop and an extended C-terminal region not present in group A, B and C MAPKs (Fig. 1A). Moreover, the 5172-bp genomic sequence of *GhMPK20* (GenBank accession number: JX470183) contains nine introns, similar to the structures of the other group D MAPKs, but greater in size than the other group D MAPKs (Fig. 1B).

To establish the intracellular localization of *GhMPK20*, a reporter gene encoding green fluorescent protein (GFP) was fused to the C-terminus of *GhMPK20* under the control of the *Cauliflower*

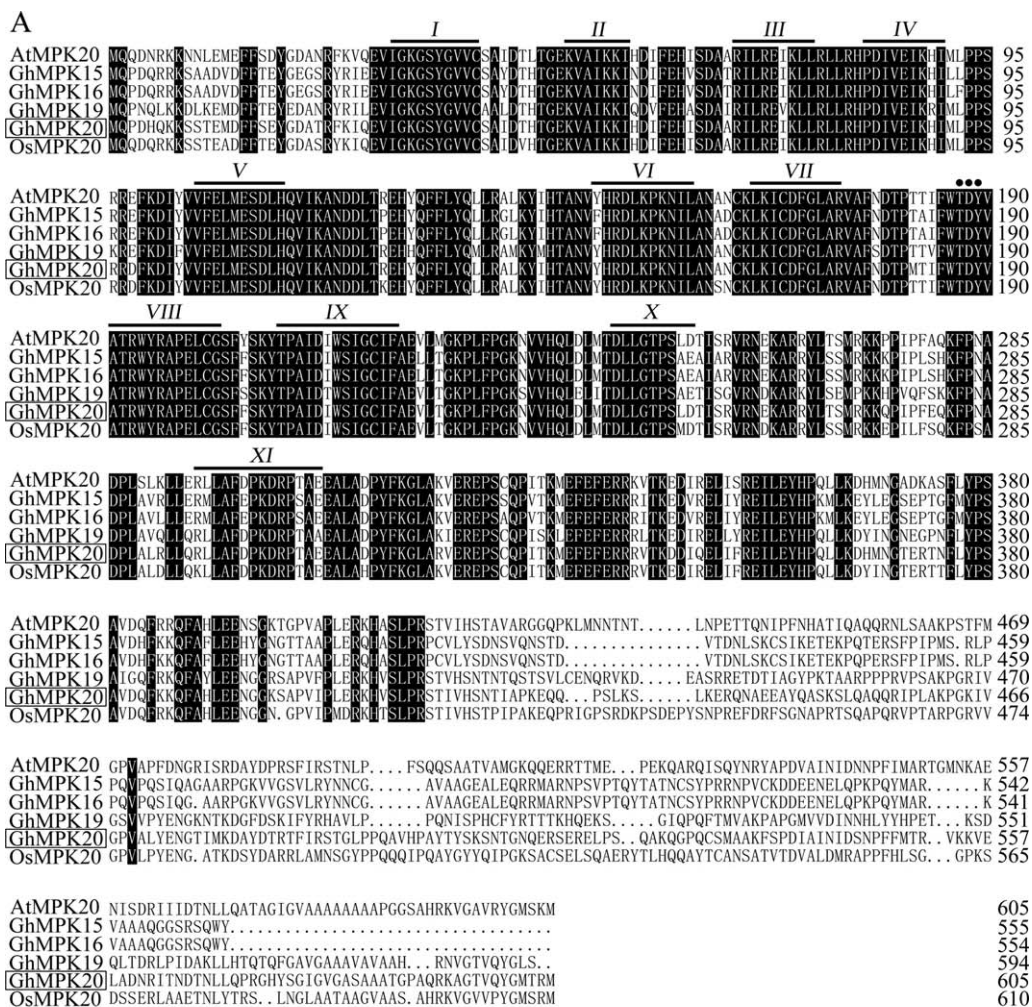


Fig. 1 Sequence analysis and genomic DNA structures of *GhMPK20*. (A) Alignment of the amino acid sequences of *GhMPK20* (HQ828072) with *AtMPK20* (AEC10180), *GhMPK15* (XP_016747991), *GhMPK16* (ADI52623), *GhMPK19* (NP_001314211) and *OsMPK20* (XP_015621247). Identical amino acids are shaded in black. The conserved subdomains are shown with numerals (I–XI) and underlined at the top of the sequences. The TDY motif is marked by a dot. (B) Comparison of the genomic DNA structure of *GhMPK20* with that of other group D mitogen-activated protein kinases (MAPKs). The legend displays the pattern of exons, introns and untranslated regions (UTRs). The scale of the x-axis indicates the length of the sequence. The abbreviations of the species names are as follows: *At*, *Arabidopsis thaliana*; *Gh*, *Gossypium hirsutum*; *Os*, *Oryza sativa*.

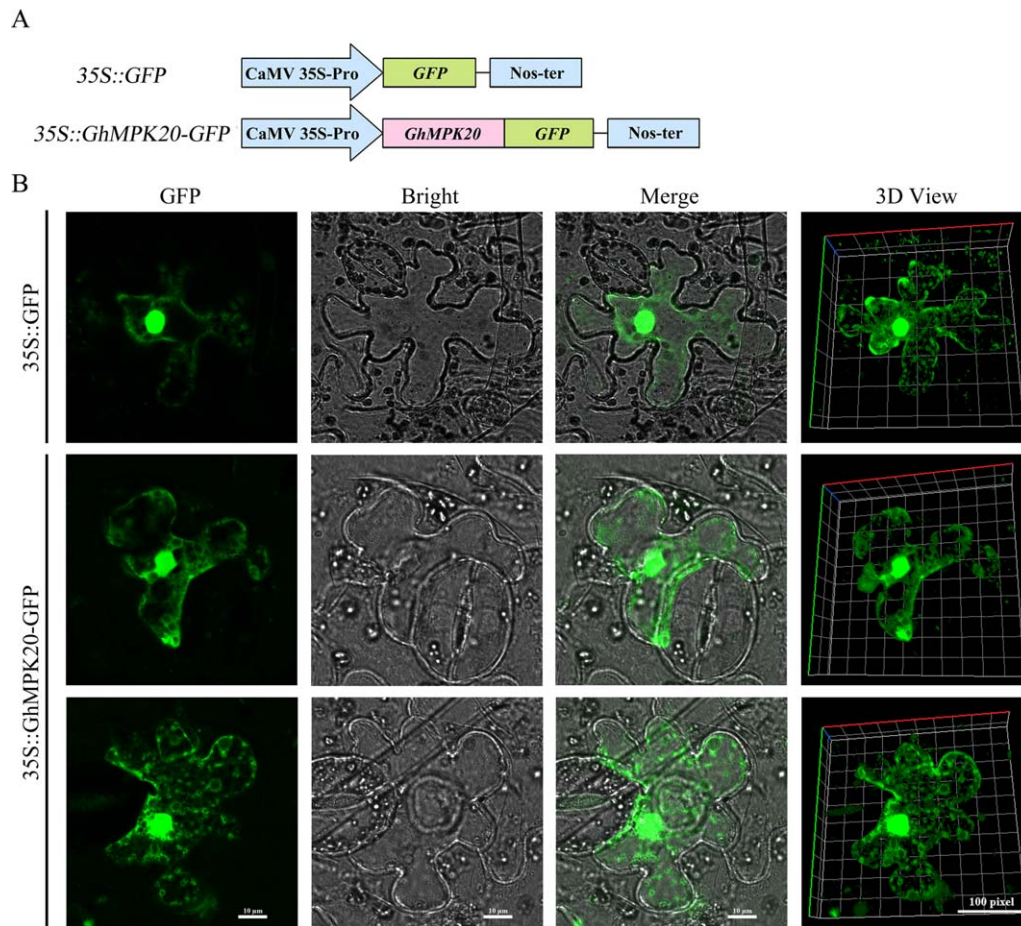


Fig. 2 Subcellular localization of GhMPK20 in *Nicotiana benthamiana* leaves. (A) Schematic diagram of the 35S::GhMPK20-GFP fusion construct and 35S::GFP construct. (B) Transient expression of the 35S::GhMPK20-GFP fusion construct and the 35S::GFP construct in *N. benthamiana* leaves. Green fluorescence was observed with an LSM 880 META confocal microscope (Carl Zeiss). GFP, green fluorescent protein.

mosaic virus 35S (CaMV35S) promoter in pBI121-GFP (Fig. 2A). The 35S::GhMPK20-GFP plasmid and the control 35S::GFP plasmid were transiently expressed separately in *N. benthamiana* leaves using *Agrobacterium* infiltration (Fig. S3, see Supporting Information). As shown in Fig. 2B, fluorescent signals from 35S::GFP and 35S::GhMPK20-GFP were distributed throughout the cytoplasm and nucleus. These results further confirm that GhMPK20 potentially functions in both the cytoplasm and nucleus.

To determine the tissue-specific expression patterns of GhMPK20, RNA was extracted from the roots, stems, leaves and cotyledons of 7-day-old cotton seedlings for quantitative reverse transcription-polymerase chain reaction (qRT-PCR). As shown in Fig. 3A, GhMPK20 was expressed in all tissues investigated in this study.

GhMPK20-silenced cotton displays enhanced resistance to *F. oxysporum*

To check whether GhMPK20 expression is induced by many disease resistance-related hormones [such as ethylene (ET), JA

and SA], cotton seedlings were separately exposed to various phytohormones. As shown in Fig. 3B,C, GhMPK20 expression was significantly enhanced after ET and JA treatments. SA treatment induced a significant decrease in the GhMPK20 expression level (Fig. 3D). These results indicate that GhMPK20 may play crucial roles in plant disease defence signal transduction pathways.

To examine whether GhMPK20 participates in cotton *F. oxysporum* resistance, virus-induced gene silencing (VIGS) was used to silence GhMPK20 in cotton. By 21 days post-infiltration (dpi), GhMPK20 mRNA levels were typically reduced (Fig. 4A). After 5 days of infection with *F. oxysporum* spore suspension, the degree of morbidity of *F. oxysporum* was determined. The degree of morbidity of *F. oxysporum* in GhMPK20-silenced (CRV::20-01 and CRV::20-02) leaves was remarkably less than that in non-silenced leaves (CRV::00) (Fig. 4B). The pathogen growth assay results showed that the *F. oxysporum* copy number in GhMPK20-silenced cotton was less than that in non-silenced cotton (Fig.

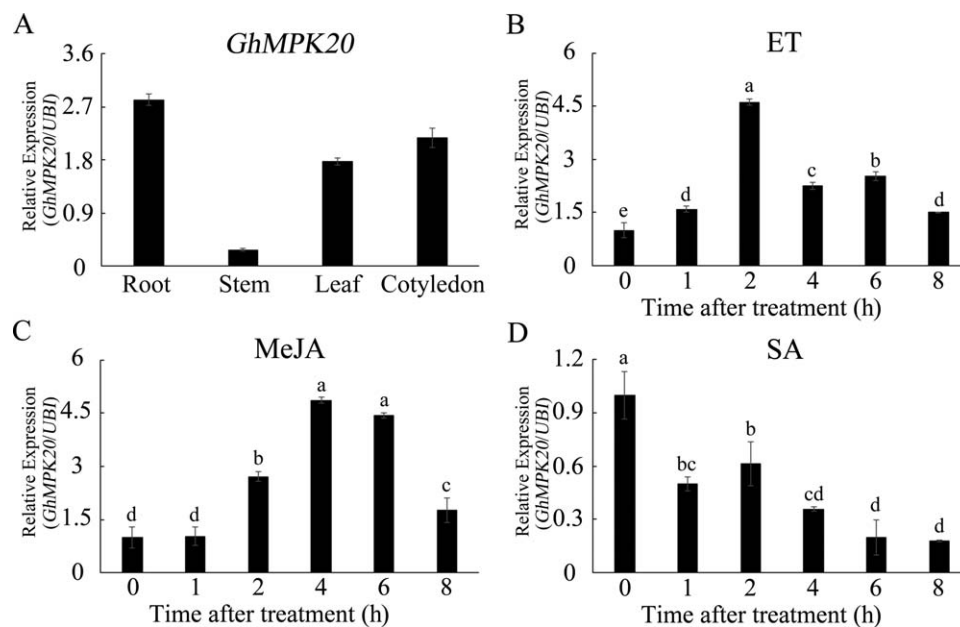


Fig. 3 Expression patterns of *GhMPK20* in different tissues and under different stress conditions. (A) Tissue-specific expression of *GhMPK20* was detected in the roots, stems, leaves and cotyledons. *GhMPK20* expression levels were analysed after cotton seedlings were separately treated with 5 mM ethylene (ET) released from ethephon (B), 100 μ M methyl jasmonate (MeJA) (C) and 10 mM salicylic acid (SA) (D). Data are presented as the mean \pm standard error (SE) of three independent experiments ($n = 6$). The letters above the columns indicate significant differences ($P < 0.05$) according to Tukey's honestly significant difference (HSD) test.

4C). In addition, the leaves of *GhMPK20*-silenced cotton accumulated less brown staining than non-silenced leaves, as demonstrated by diaminobenzidine (DAB) staining (Fig. 4B). To elucidate the mechanism underlying this enhanced resistance, the expression levels of SA-mediated defence pathway genes and pathogenesis-related (*PR*) genes were examined. The SA-mediated genes and *PR* genes showed much higher expression levels in *GhMPK20*-silenced cotton than in non-silenced leaves after *F. oxysporum* infection (Fig. 4D). These results show that *GhMPK20* silencing enhances *F. oxysporum* resistance in cotton.

GhMPK20*-overexpressing plants display enhanced sensitivity to *F. oxysporum

To further detect the biological function of *GhMPK20* in disease resistance, transgenic *N. benthamiana* plants overexpressing *GhMPK20* were generated, and three independent overexpressing lines (10#, 13# and 17#, named OE1, OE2 and OE3, respectively) were selected (Fig. S4, see Supporting Information). The T3 generations of these three transgenic plants were used for further functional study.

After plants were infected with *F. oxysporum* for 5 days, the leaves of overexpressing (OE) plants showed more serious wilting symptoms and chlorosis than did vector control (Vec) plants (Fig. 5A). Histochemical staining with trypan blue and DAB showed that OE leaves accumulated more blue and brown staining than did Vec leaves (Fig. 5A). The expression levels of

SA-mediated defence pathway genes and *PR* genes were also examined. As shown in Fig. 5B, the expression levels of all the tested genes were significantly decreased in OE leaves. These results indicate that *GhMPK20*-overexpressing plants display enhanced susceptibility to *F. oxysporum*.

***GhMPK20* interacts with *GhMCK4* in vitro and in vivo**

MAPKKs are potential upstream genes of MAPKs (MAPK Group, 2002). To investigate the upstream component of *GhMPK20*, based on our previous studies and the cotton genome, the interactions between *GhMPK20* and some cotton MKKs [such as the A group MKK gene *GhMCK6* (Gene ID: 107932005), B group MKK gene *GhMCK3* (GenBank accession number: HQ828070), C group MKK genes *GhMCK4* (GenBank accession number: FJ966886) and *GhMCK5* (GenBank accession number: HQ637469), and D group MKK gene *GhMCK9* (GenBank accession number: HQ651069)] were detected using yeast two-hybrid assays. The yeast two-hybrid assay results showed that only the positive control clone and the clone co-transformed with *GhMPK20* and *GhMCK4* grew well on SD medium DDO and QDO/X (SD, synthetically defined medium; SD medium DDO, SD medium without Leu and Trp; SD medium QDO/X, SD medium with X-a-gal and without Ade, His, Leu, Trp) plates, indicating that *GhMCK4* may be the upstream component of *GhMPK20* (Fig. 6A). The interaction between *GhMPK20* and *GhMCK4* was further confirmed using the bimolecular fluorescence complementation (BiFC) system, in which

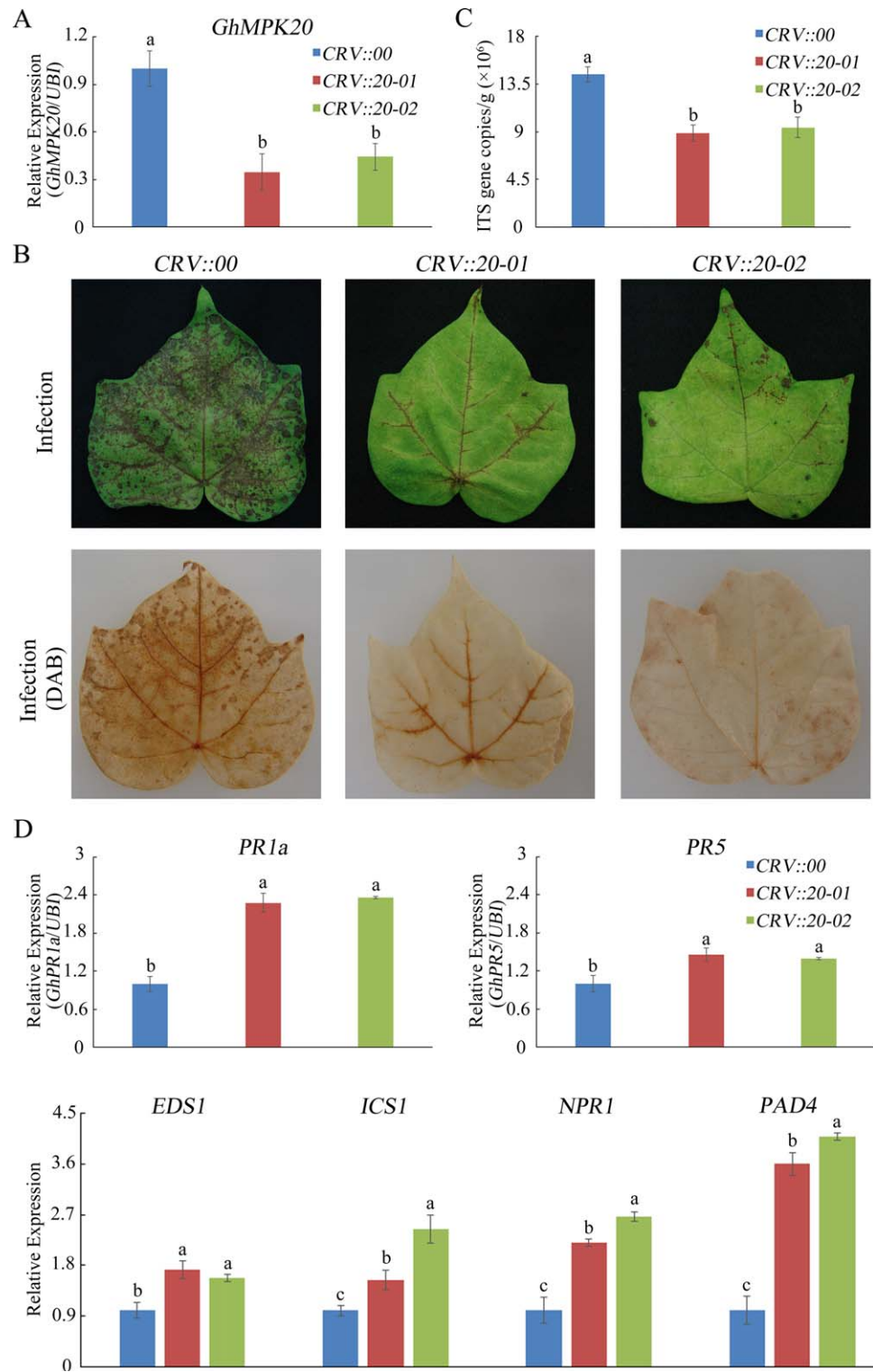


Fig. 4 Silencing of *GhMPK20* in cotton increases the tolerance to *Fusarium oxysporum*. (A) *GhMPK20* expression levels in *GhMPK20*-silenced cotton plants. (B) Representative phenotypes of *GhMPK20*-silenced cotton after infection with *F. oxysporum* for 5 days. DAB, diaminobenzidine. (C) Pathogen accumulation level in *GhMPK20*-silenced plants after infection with *F. oxysporum* for 5 days. ITS indicates the nuclear ribosomal DNA internal transcribed spacer (ITS) sequences of fungi. (D) Expression level of salicylic acid (SA)-mediated defence pathway genes and pathogenesis-related (*PR*) genes in *GhMPK20*-silenced cotton plants after infection with *F. oxysporum* for 5 days. The error bars in (A), (C) and (D) indicate the mean \pm standard error (SE) of three independent experiments ($n = 9$). The letters above the columns represent significant differences ($P < 0.05$) based on Tukey's honestly significant difference (HSD) test.

GhMPK20-yellow fluorescent protein (YFP)^C and *GhMKK4*-YFP^N were co-transformed into onion epidermal cells through particle bombardment. In accordance with the localization of *GhMPK20* (Fig. 2) and *GhMKK4* (Li *et al.*, 2014), the fluorescent signal was

detected in both the cytoplasm and nucleus (Fig. 6B). Furthermore, co-immunoprecipitation (Co-IP) assays verified the interaction between *GhMPK20* and *GhMKK4*. The Co-IP result showed that *GhMKK4*-FLAG could be immunoprecipitated by *GhMPK20*-

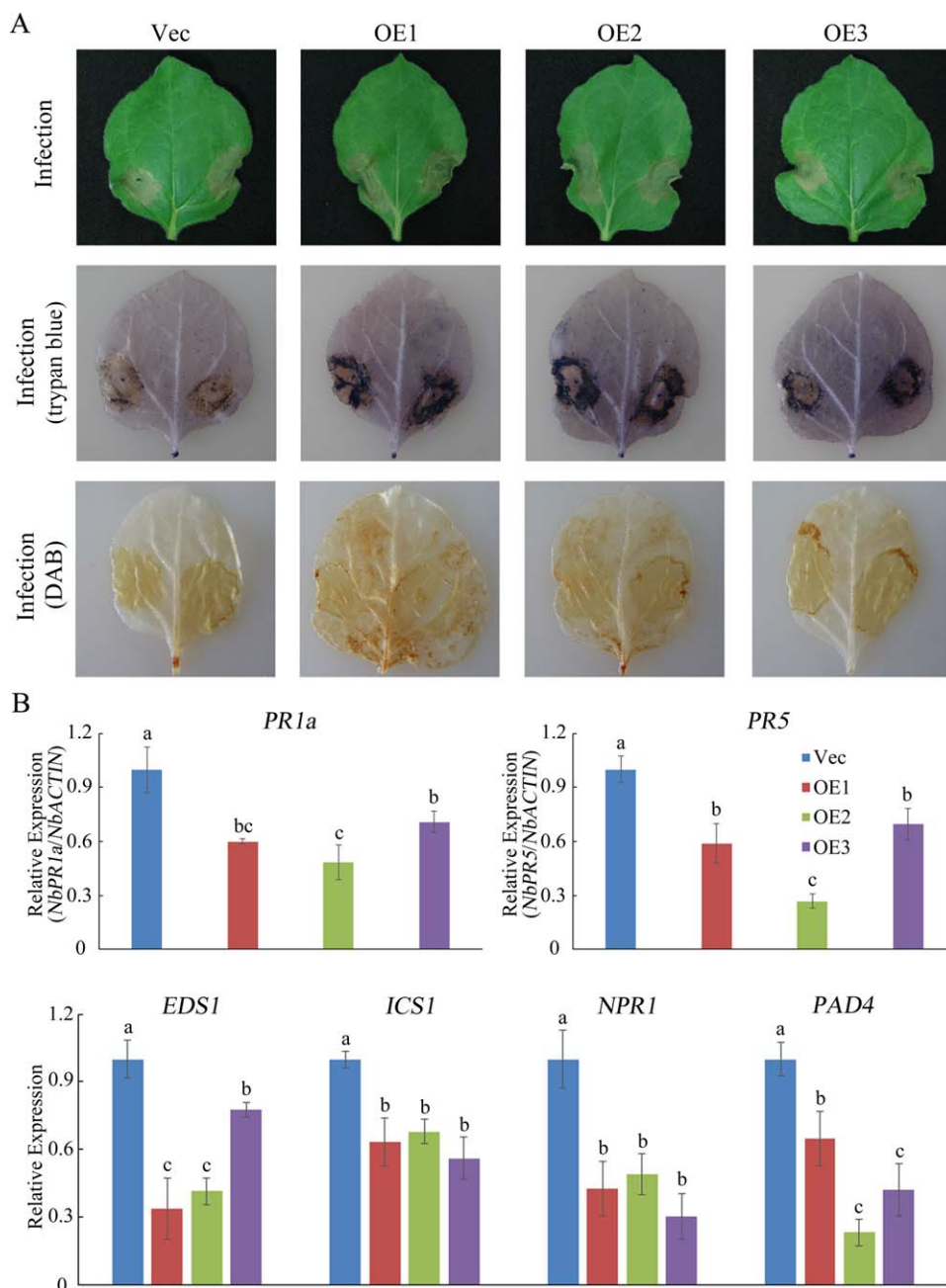


Fig. 5 *GhMPK20* overexpression reduces the tolerance to *Fusarium oxysporum* in transgenic *Nicotiana benthamiana*. (A) Representative phenotypes of *GhMPK20*-overexpressing plants after infection with *F. oxysporum* for 5 days. DAB, diaminobenzidine. (B) Expression levels of salicylic acid (SA)-mediated defence pathway genes and pathogenesis-related (PR) genes in *GhMPK20*-overexpressing *N. benthamiana* after infection with *F. oxysporum* for 5 days. Data are presented as the mean \pm standard error (SE) of three independent experiments ($n = 9$). The letters above the columns indicate significant differences ($P < 0.05$) based on Tukey's honestly significant difference (HSD) test.

MYC in protoplasts (Fig. 6C). These results demonstrate that *GhMPK20* interacts with *GhMCK4* *in vitro* and *in vivo*.

GhMCK4*-silenced cotton displays enhanced resistance to *F. oxysporum

To test whether *GhMCK4* has functions similar to those of *GhMPK20*, we used VIGS to silence *GhMCK4* in cotton. After cotton plants were infiltrated with *Agrobacterium* for 3 weeks, *GhMCK4* expression was significantly reduced in *CRV::GhMCK4*

cotton plants (Fig. S5, see Supporting Information). Then, *CRV::00* and *CRV::GhMCK4* (*CRV::4-01* and *CRV::4-02*) were root-wounded and placed in an *F. oxysporum* spore suspension. After these plants were infected with *F. oxysporum* for 5 days, the *CRV::GhMCK4* (*CRV::4-01*, *CRV::4-02*) plants showed resistance phenotypes and presented less brown staining than *CRV::00* leaves, as determined by DAB staining (Fig. 7A). Furthermore, the SA-mediated genes and PR genes showed the same expression profiles between *CRV::GhMCK4* and *CRV::GhMPK20* plants after *F. oxysporum* infection for 5 days (Fig. 7B).

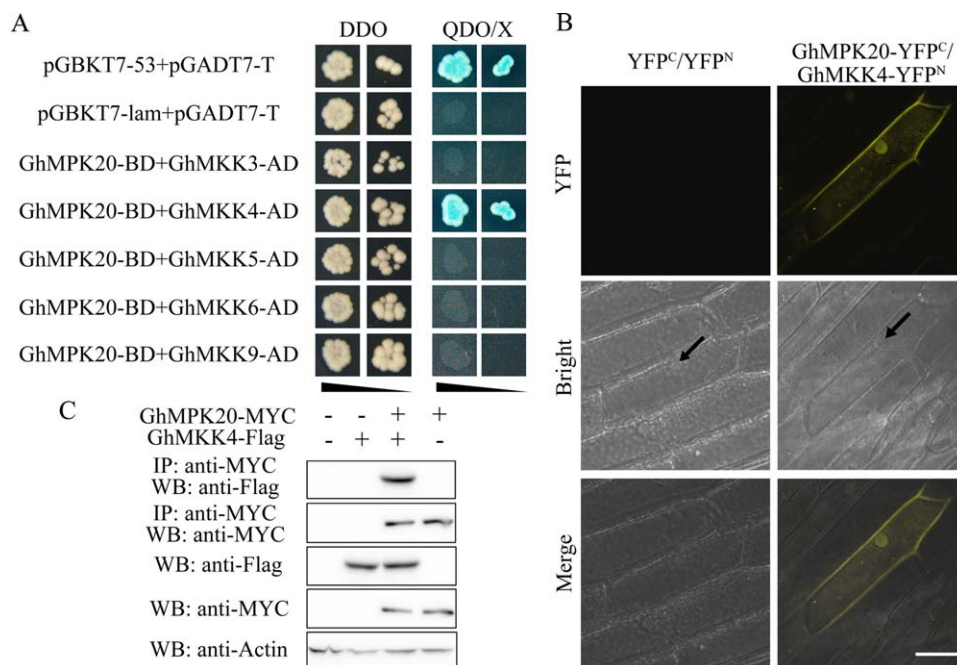


Fig. 6 Interaction between GhMPK20 and GhMKK4. (A) GhMPK20 specifically interacts with GhMKK4 according to the yeast two-hybrid (Y2H) system assay results. The indicated BD and AD fusion constructs were co-transformed into the Y2H Gold yeast strain and grown on the SD media DDO and QDO/X. (B) The interaction between GhMPK20 and GhMKK4 was confirmed by bimolecular fluorescence complementation (BiFC) experiments. GhMPK20-YFP^C and GhMKK4-YFP^N fusion constructs were co-transformed into onion epidermal cells using the particle bombardment method. Yellow fluorescence was observed with an LSM 510 META confocal microscope (Carl Zeiss). Arrowheads indicate nuclei. Bar, 50 μ m. YFP, yellow fluorescent protein. (C) Co-immunoprecipitation analysis was performed using MYC antibody in cotton protoplasts. GhMPK20-MYC and GhMKK4-FLAG fusion constructs were co-transformed into cotton protoplasts. Western blot analysis shows protein expression levels. SD, synthetically defined medium; SD medium DDO, SD medium without Leu and Trp; SD medium QDO/X, SD medium with X-a-gal and without Ade, His, Leu, Trp.

GhMKK4–GhMPK20 function upstream of GhWRKY40 under *F. oxysporum* infection

Many studies have shown that WRKY TFs are amongst the most important substrates for MAPK cascades (Ishihama and Yoshioka, 2012). Previously, we have shown that *GhWRKY40* is induced by fungal disease and GhWRKY40 interacts with GhMPK20 (Wang *et al.*, 2014). In this study, the yeast two-hybrid assay result showed that the positive control clone and the clone co-transformed with GhMPK20 and GhWRKY40 grew well on SD medium DDO and QDO/X plates (Fig. 8A). Co-IP also showed that GhWRKY40-FLAG could be immunoprecipitated by GhMPK20-MYC in protoplasts (Fig. 8B).

To prove that these three signalling elements are indeed from the same cascade, a Phos-tag-based method was used in the phosphorylation assay. Phos-tag, together with a chelated divalent cation, such as Mn^{2+} , can bind phosphate groups (Longoni *et al.*, 2015), and phosphorylated proteins can be resolved from their non-phosphorylated forms based on differences in their migration rates (Bekešová *et al.*, 2015). As shown in Fig. S6 (see Supporting Information), the phosphorylation levels of GhMPK20 were remarkably higher in cotton protoplasts co-transformed with GhMKK4-FLAG and GhMPK20-MYC than in those transformed

with only GhMPK20-MYC (Fig. S6A). Furthermore, the phosphorylation levels of GhWRKY40 were higher in cotton protoplasts co-transformed with GhMPK20-MYC and GhWRKY40-FLAG than in those transformed with only GhWRKY40-FLAG (Fig. S6B).

To investigate whether *GhWRKY40* expression is induced by *F. oxysporum*, cotton seedlings were exposed to *F. oxysporum*. *GhWRKY40* transcript accumulation was typically elevated at the different time points following *F. oxysporum* infection (Fig. S7, see Supporting Information). To identify the function of *GhWRKY40* on *F. oxysporum* infection, we used VIGS to silence *GhWRKY40* in cotton (Fig. 8C). Five days after *F. oxysporum* infection, the leaves from *CRV::GhWRKY40* exhibited milder wilting symptoms and chlorosis than did *CRV::00* cotton (Fig. 8E). DAB staining showed that the *CRV::GhWRKY40* leaves accumulated less brown staining than *CRV::00* leaves (Fig. 8E).

To confirm that the function of GhMKK4–GhMPK20 is required for *F. oxysporum*-induced *GhWRKY40* expression. *GhMKK4*-silenced and *GhMPK20*-silenced leaves were infected with *F. oxysporum*. Compared with *CRV::00* control plants, *GhWRKY40* expression did not show obvious changes in *GhMKK4*-silenced or *GhMPK20*-silenced cotton plants after *F. oxysporum* infection (Fig. 8D,F). Furthermore, *GhMPK20* expression was increased in the leaves of *CRV::00* cotton plants, whereas that in *CRV::GhMKK4* plants

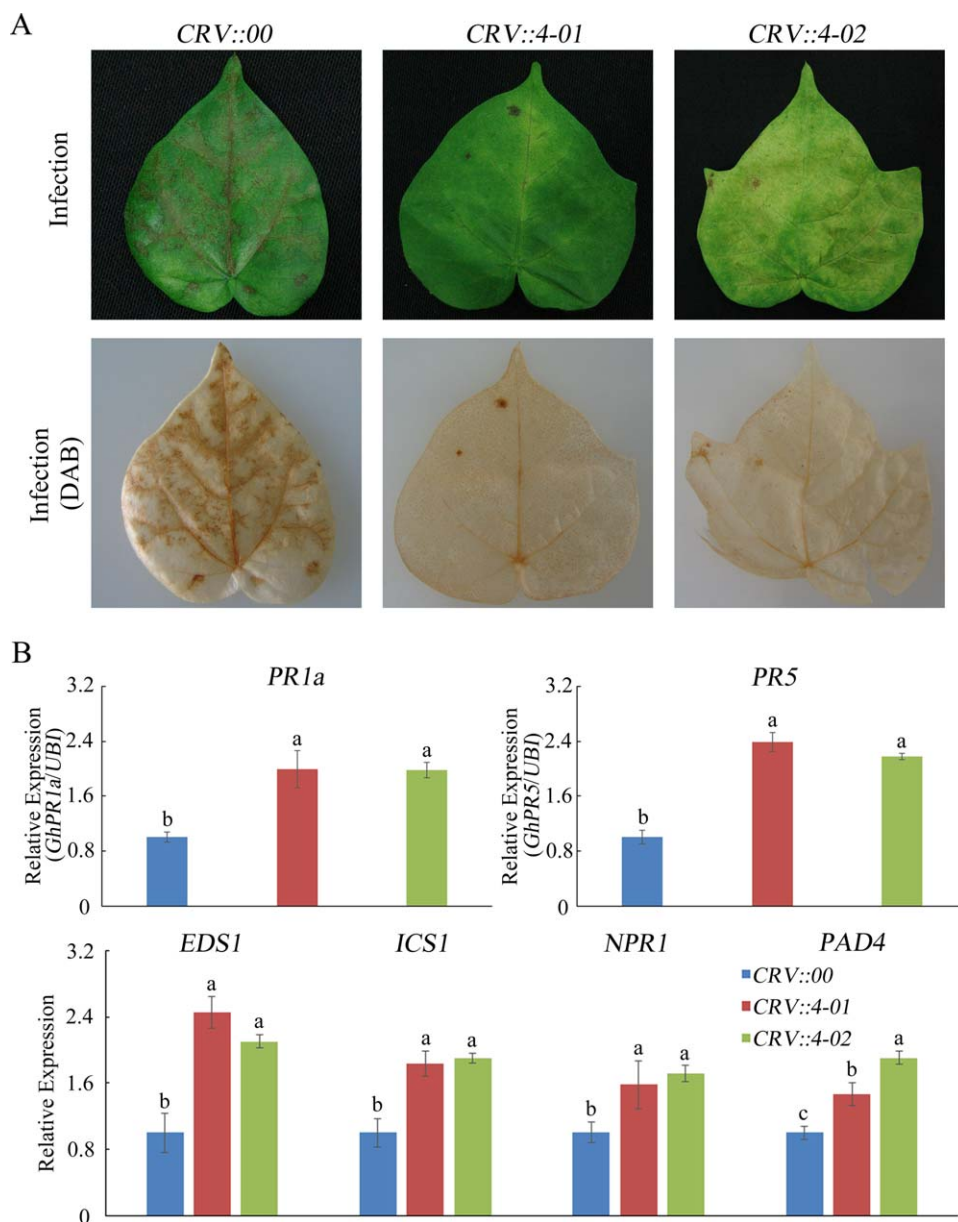


Fig. 7 Silencing of *GhMCK4* in cotton increases the tolerance to *Fusarium oxysporum*. (A) Representative phenotypes of *GhMCK4*-silenced cotton after infection with *F. oxysporum* for 5 days. DAB, diaminobenzidine. (B) Expression levels of salicylic acid (SA)-mediated defence pathway genes and pathogenesis-related (*PR*) genes in *GhMCK4*-silenced cotton after infection with *F. oxysporum* for 5 days. Data are presented as the mean \pm standard error (SE) of three independent experiments ($n = 9$). The letters above the columns indicate significant differences ($P < 0.05$) based on Tukey's honestly significant difference (HSD) test.

showed no obvious changes after *F. oxysporum* infection (Fig. 8F). These results suggest that the function of GhMCK4–GhMCK20 is essential for *F. oxysporum*-induced *GhWRKY40* expression.

DISCUSSION

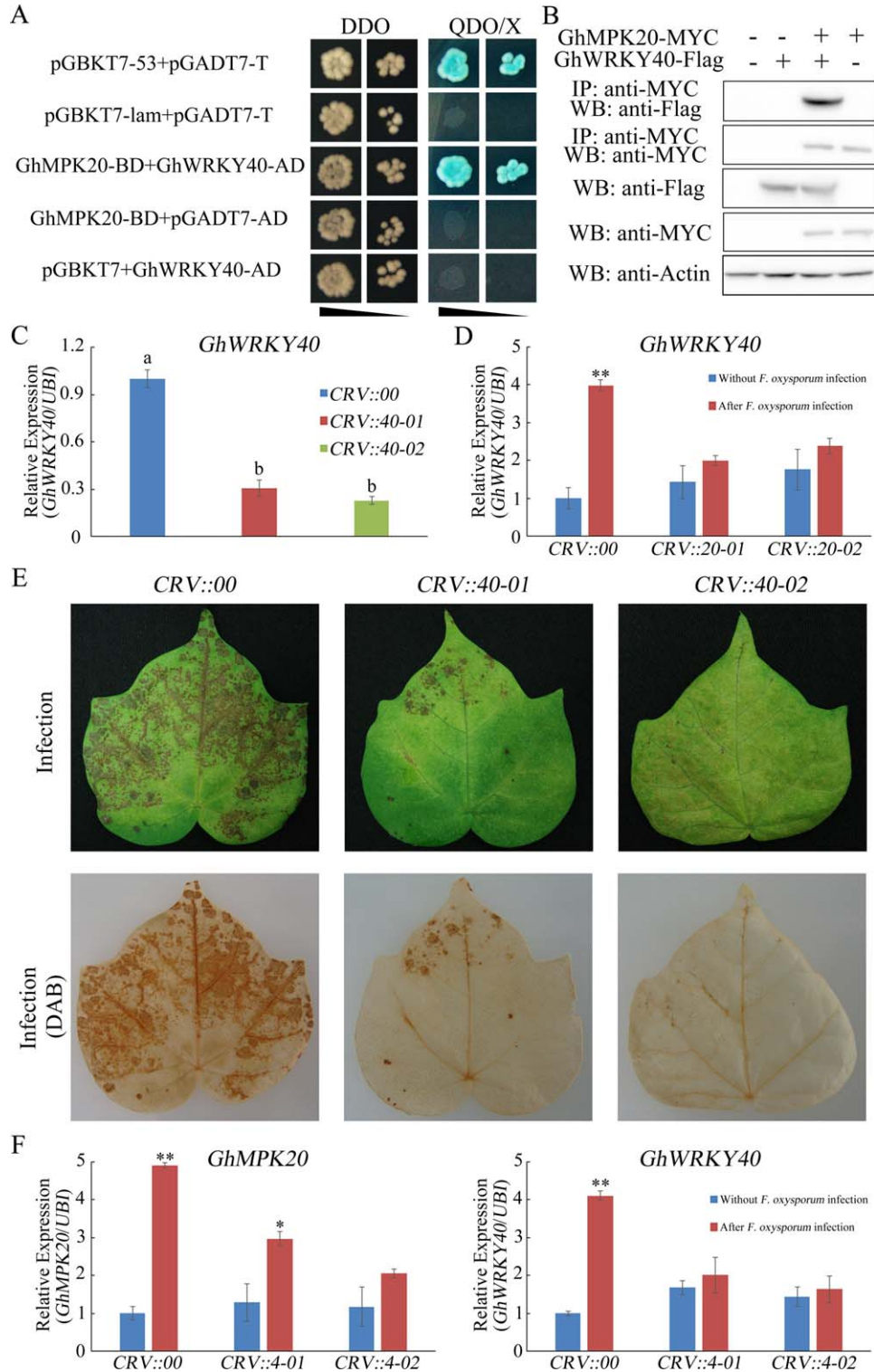
MAPK pathways are amongst the most important signal transduction pathways in plants, and many MAPK genes have been identified; however, information regarding the functions of group D MAPKs remains limited. In this study, *GhMCK20*, a new group D MAPK gene, was identified in *G. hirsutum*, and silencing of *GhMCK20* in cotton enhanced resistance to *F. oxysporum*.

GhMCK20 possesses the typical features of group D MAPKs, such as the TDY activation motif, an extended C-terminal region

and the lack of a CD domain (Fig. 1) (MAPK group). The first identified function of group D MAPKs is enhanced resistance to fungal and bacterial infections by the overexpression of *OsBWMK1* through constitutive *PR* gene expression (Cheong *et al.*, 2003). Maize *ZmMPK17* is involved in multiple stress responses, such as cold, osmotic stress and SA-mediated pathogen defence (Pan *et al.*, 2012). Moreover, active AtMPK18 can be dephosphorylated by PHS1 in the cytoplasm to regulate cortical microtubule functions (Walia *et al.*, 2009). In cotton, *GhMCK20* has many homologous genes, including *GhMCK15* (GenBank accession number: XP_016747991), *GhMCK16* (GenBank accession number: ADI52623) and *GhMCK19* (GenBank accession number: NP_001314211) (Fig. 1). However, the

functions of TDY MAPKs in cotton are unclear. In our previous studies, cotton *GhMPK16* enhanced resistance to fungal (*Colletotrichum nicotianae* and *Alternaria alternata*) and bacterial (*Pseudomonas solanacearum*) pathogens in transgenic plants

by rapidly inducing the expression of some PR genes (Shi *et al.*, 2011). In this study, *GhMPK20* was shown to differ from other group D MAPKs and conferred sensitivity to *F. oxysporum* stress in transgenic plants (Fig. 5).



Most of the plant MAPKs reported recently play important roles in pathogen resistance, whereas few MAPKs have been identified as negative effectors. AtMPK4, which can be activated by AtMKK1 and AtMKK2, is a negative regulator of the innate immune response in plants (Gao *et al.*, 2008). Furthermore, functional analysis of *Arabidopsis* immune-related MAPKs identified a negative role for MPK3 in the regulation of defence gene expression, SA accumulation and disease resistance to *P. syringae* (Frey *et al.*, 2014). The present study revealed that *GhMPK20* expression was highly induced in cotton after infection with *F. oxysporum*, suggesting that *F. oxysporum* might activate *GhMPK20* to inhibit the defence response during infection. Furthermore, VIGS of *GhMPK20* in cotton enhanced the tolerance to *F. oxysporum* by increasing the expression of some *PR* and SA-related genes (Fig. 4). As a result of experimental condition limitations, cotton transformation is very difficult. Considering the easy transformation and convenience of studying *F. oxysporum* resistance, gain-of-function analysis was first performed by heterologous ectopic expression in *N. benthamiana*. Overexpression of *GhMPK20* in *N. benthamiana* resulted in opposite phenotypes for *GhMPK20*-silenced cotton. These data provide novel information and enrich our understanding of the functions of group D MAPKs in cotton.

In *Arabidopsis*, the AtMEKK1–AtMKK4/5–AtMPK3/6 cascade is involved in the regulation of the plant innate immune response, and the AtYODA–AtMKK4/5–AtMPK3/6 module plays critical roles in pathogen signalling and stomatal development (MAPK Group, 2002; Rodriguez *et al.*, 2010). In addition to the model plant *Arabidopsis*, some cascades in other plants, such as tomato, tobacco, rice and apple, have also been identified (Kishi-Kaboshi *et al.*, 2010; Pedley and Martin, 2004; Wang *et al.*, 2010; Yang *et al.*, 2001). However, the components of these cascades require further study because they are largely incomplete. In our previous studies, we reported that *GhWRKY40* is a potential downstream gene of *GhMPK20* (Wang *et al.*, 2014). Here, based on the yeast two-hybrid, BiFC and Co-IP analyses, a MAPK cascade composed of GhMCK4, GhMPK20 and GhWRKY40 was identified (Figs 6 and 8). *GhMCK4* has been shown to enhance disease susceptibility by disrupting the SA signalling pathway (Li *et al.*, 2014). *GhWRKY40* overexpression also decreased the resistance of transgenic plants to pathogen infection and

decreased the accumulation of *PR1* transcripts (Wang *et al.*, 2014). In this study, silencing of *GhMCK4*, *GhMPK20* and *GhWRKY40* in cotton enhanced the resistance to *F. oxysporum*. Furthermore, we found that the function of GhMCK4–GhMPK20 is essential for *F. oxysporum*-induced *GhWRKY40* expression (Fig. 8).

SA has been identified as one of the most crucial signalling molecules in the mediation of plant defence responses (Vlot *et al.*, 2009). After pathogen infection, SA rapidly accumulates and activates the plant innate immunity response (Gao *et al.*, 2017). *PR1* is a key marker gene of SA signalling. High expression levels of *PR1* indicate that SA signalling has been activated (He *et al.*, 2007). *NPR1* is another key marker of SA signalling, and an *npr1* mutant was found to be SA insensitive, as it exhibited enhanced susceptibility to many bacterial and fungal pathogens (Delaney *et al.*, 1995; Glazebrook *et al.*, 1996). An *eds5* mutant also enhanced disease susceptibility by inhibiting SA synthesis, and this phenotype could be rescued by the addition of SA (Rogers and Ausubel, 1997). In this study, we noticed that SA-related genes, such as *EDS1*, *ICS1*, *NPR1*, *PAD4* and *PR1*, were significantly induced after *F. oxysporum* infection in *GhMCK4*-silenced (Fig. 7), *GhMPK20*-silenced (Fig. 4) and *GhWRKY40*-silenced (Fig. S8, see Supporting Information) cotton. Furthermore, as shown in Fig. S10 (see Supporting Information), after *F. oxysporum* infection for 5 days, the degree of *F. oxysporum* morbidity was remarkably lower after the external application of SA (10 mM), although the phenotype was not rescued completely. These results indicate that the GhMCK4–GhMPK20–GhWRKY40 cascade disrupts the SA signalling pathway and/or inhibits SA synthesis. Ding *et al.* (2011) have reported that, although SA- and JA-mediated defence signalling pathways are known to have an antagonistic relationship, synergy between the two is coordinated in resistance-related early molecular events. The sequential induction of SA- and JA-mediated pathways would be an effective coordination mechanism of the two antagonistic pathways (Ding *et al.*, 2011). Based on our results, we speculate that the GhMCK4–GhMPK20–GhWRKY40 cascade negatively regulates *F. oxysporum* resistance by disrupting this coordination.

Fusarium wilt disease has devastating effects on cotton, causing substantial crop losses in most of the major cotton-

Fig. 8 Function of GhMCK4–GhMPK20 is essential for *Fusarium oxysporum*-induced *GhWRKY40* expression. (A) GhMPK20 interacts with GhWRKY40 according to the yeast two-hybrid (Y2H) system assay results. The indicated BD and AD fusion constructs were co-transformed into the Y2H Gold yeast strain and grown on the SD media DDO and QDO/X. (B) Co-immunoprecipitation (Co-IP) analysis was performed using MYC antibody in cotton protoplasts. GhMPK20-MYC and GhWRKY40-FLAG fusion constructs were co-transformed into cotton protoplasts. Western blot analysis shows protein expression levels. (C) *GhWRKY40* expression levels in *GhWRKY40*-silenced cotton plants. The data are presented as the mean \pm standard error (SE) of three independent experiments ($n = 9$). The letters above the columns represent significant differences ($P < 0.05$) based on Tukey's honestly significant difference (HSD) test. (D) *GhWRKY40* expression levels in *GhMPK20*-silenced cotton plants with or without *F. oxysporum* infection. The error bars indicate the mean \pm SE of three independent experiments ($n = 9$). Asterisks above the lines indicate significant differences ($*P < 0.05$, $**P < 0.01$) based on Tukey's HSD test. (E) Representative phenotypes of *GhWRKY40*-silenced cotton after infection with *F. oxysporum* for 5 days. DAB, diaminobenzidine. (F) *GhMPK20* and *GhWRKY40* expression levels in *GhMCK4*-silenced cotton plants with or without *F. oxysporum* infection. The error bars indicate the mean \pm SE of three independent experiments ($n = 9$). Asterisks above the lines indicate significant differences ($*P < 0.05$, $**P < 0.01$) based on Tukey's HSD test. SD, synthetically defined medium; SD medium DDO, SD medium without Leu and Trp; SD medium QDO/X, SD medium with X-a-gal and without Ade, His, Leu, Trp.

producing areas worldwide (Wang *et al.*, 2006). Many studies have reported that Fusarium wilt is a component of a disease complex with root-knot nematodes and that *F. oxysporum* can secrete many enzymes to break the physical barriers and anti-fungal compounds of plants (Pietro *et al.*, 2003; Wang *et al.*, 2006). However, the pathogenic mechanism of *F. oxysporum* and the mechanism by which *F. oxysporum* overcomes plant defence responses are unclear. In this study, we report a new strategy by which *F. oxysporum* attacks plants. After root invasion and vascular colonization, the MAPK cascade, composed of GhMCK4, GhMPK20 and GhWRKY40, is affected by *F. oxysporum*. This MAPK cascade may disrupt the SA-related defence pathway by decreasing the expression of some SA-related genes and *PR* genes (Figure S9). Our results compensate for deficiency of knowledge in the pathogenic process of *F. oxysporum* in cotton and provide an important scientific basis for the formulation of Fusarium wilt prevention strategies.

EXPERIMENTAL PROCEDURES

Plant materials, growth conditions and stress treatments

Cotton (*G. hirsutum* L. cv. lumian 22) seedlings were planted in hydroponic cultures and received 16 h of continuous light followed by 8 h of darkness per 24-h period under glasshouse conditions at 26 ± 1 °C. For expression pattern analyses, uniform cotton seedlings were sprayed with ET released from ethephon (5 mM), JA (100 μ M) and SA (10 mM) or inoculated with *F. oxysporum* conidial suspensions (10^6 conidia/mL) using the root-dip method. Transgenic and vector control (Vec) *N. benthamiana* seedlings were planted in soil under a 16-h light/8-h dark photoperiod at 25 ± 1 °C. For *F. oxysporum* infections performed on cotton plants, the seedlings were inoculated with *F. oxysporum* conidial suspensions (10^6 conidia/mL) using the root-dip method. In addition, the *F. oxysporum* conidial suspensions (10^6 conidia/mL) were injected into the leaves of GhMPK20-overexpressing *N. benthamiana* using syringes. The treated materials were collected and frozen at -80 °C for RNA extraction. Each treatment was repeated at least three times.

GhMPK20 cloning, sequence analyses, vector construction and genetic transformation

The methods of cloning GhMPK20 cDNA and genomic sequences were performed as described previously (Zhang *et al.*, 2012). Amino acid sequence alignments and the phylogenetic tree of GhMPK20 and other MAPKs were produced by DNAMAN and Molecular Evolutionary Genetics Analysis (MEGA) software 4.0, respectively. The ORF of GhMPK20 was cloned and inserted into the vector pRI 201-AN (TaKaRa, Japan) under the control of a CaMV35S promoter. GhMPK20-overexpressing *N. benthamiana* plants were obtained according to previously described procedures (Zhang *et al.*, 2011). The primers used in this study are shown in Table S1 (see Supporting Information).

Subcellular localization of GhMPK20

To achieve transient expression, the recombinant plasmids 35S::GhMPK20-GFP and 35S::GFP were transformed into *Agrobacterium tumefaciens* strain GV3101. After *A. tumefaciens* was cultured overnight, the cultures were pelleted and resuspended [optical density at 600 nm (OD_{600}) = 1] in infiltration medium (10 mM $MgCl_2$, 10 mM MES-NaOH, pH 3.8, 200 μ M acetosyringone). The leaves of 5-week-old *N. benthamiana* were used for transient expression. The fluorescent signals were observed with an LSM 880 META confocal microscope (Carl Zeiss, Germany).

RNA extraction and expression analyses of GhMPK20

The modified cetyl-trimethyl-ammonium bromide (CTAB) method (Wang *et al.*, 2011) or TRIzol reagent (Invitrogen, Carlsbad, CA, USA) was used to extract total RNA from all experimental samples. Subsequently, first-strand cDNA was synthesized using EasyScript First-Strand cDNA Synthesis SuperMix (Transgen, Beijing, China). The expression patterns of target genes for functional assays were analysed by qRT-PCR. Reactions were performed in a 20- μ L reaction volume using a CFX96™ Real-time Detection System (Bio-Rad) and Bestar SybrGreen qPCR Mastermix (DBI, Germany). The following PCR program was used: pre-denaturation at 95 °C for 2 min; 40 cycles of 95 °C for 10 s, 55 °C for 30 s and 72 °C for 30 s; and a final melt cycle from 55 to 98 °C. The *G. hirsutum ubiquitin (UBI)* or *N. benthamiana β -actin* gene was used as the standard control.

Agrobacterium-mediated VIGS

The method for VIGS was performed according to Gu *et al.* (2014). The fragments of GhMPK20, GhMCK4 and GhWRKY40 were inserted into the pCLCrV-A vector. The primers used are shown in Table S1. The recombinant vectors pCLCrV-A and pCLCrV-B were transformed into *A. tumefaciens* strain EHA105. After *A. tumefaciens* was cultured overnight, the cultures were pelleted and resuspended (OD_{600} = 1) in infiltration medium as described above. The *Agrobacterium* suspensions containing pCLCrV-A or pCLCrV-B were mixed equally and inoculated into two fully expanded cotton cotyledons after incubation for 3 h. The leaves of the inoculated cotton plants were used for assays 3 weeks after inoculation. Each assay was performed using at least three independent biological replicates.

Yeast two-hybrid, BiFC and Co-IP assays

The interaction between GhMPK20 and cotton MKKs (GhMCK3, GhMCK4, GhMCK5, GhMCK6 or GhMCK9) or GhWRKY40 was detected with the Matchmaker Gold Yeast Two-Hybrid System (Clontech, Japan) and the BiFC system as described previously (Li *et al.*, 2013). For the yeast two-hybrid system, the ORF region of GhMPK20 was cloned and fused to the GAL4 DNA-binding domain in the bait plasmid pGBKT7. The ORF regions of GhWRKY40 or MKKs were separately cloned into the GAL4 activation domain in the prey vector pGADT7. The appropriate combinations of two plasmids amongst these plasmids were co-transformed into the yeast two-hybrid Gold strain and plated on DDO (SD medium without Leu and Trp [SD/-Leu/-Trp]) medium. Then, the positive clones were grown on the selective SD medium (QDO/X, SD medium with X-a-gal and without Ade, His, Leu, Trp [SD/-Ade/-His/-Leu/-Trp with X-a-gal]).

For the BiFC system, *GhMPK20* and *GhMCK4* were fused into pUC-SPYCE-35S and pUC-SPYNE-35S, respectively. Subsequently, these two recombinant plasmids were co-transformed into onion epidermal cells using the particle bombardment method. The fluorescent signal was detected with a confocal microscope (LSM 510 META; Carl Zeiss).

For the Co-IP assay, cotton seedlings were germinated under 16 h of continuous light followed by 8 h of darkness per 24-h period. Cotton cotyledons were used to prepare protoplasts as described by Chen *et al.* (2017). Cotyledons were cut into 0.5-mm strips and immediately transferred into 10 mL of enzyme solution [2.0% cellulase R10, 0.4% macerozyme R10, 0.6 M mannitol, 10 mM MES (pH 5.7), 20 mM KCl, 10 mM CaCl₂ and 0.1% bovine serum albumin (BSA)] to digest at 25 °C after being vacuum prepared for 30 min. The following steps and protoplast transformation were performed as described by Yoo *et al.* (2007). *GhMPK20* was inserted into the pGreenII 62-MYC vector (GhMPK20-MYC), and *GhMCK4* or *GhWRKY40* was fused into the pZP211-Flag vector (GhMCK4-FLAG or GhWRKY40-FLAG). The Co-IP assay was performed using a ProFound c-MYC Tag IP/Co-IP kit (Thermo Fisher) according to previously described procedures (Wang C *et al.*, 2016).

Phos-tag sodium dodecylsulfate-polyacrylamide gel electrophoresis (SDS-PAGE)

GhMCK4-FLAG, GhMPK20-MYC and GhWRKY40-FLAG were transformed into cotton protoplasts as described above. Total proteins were extracted from leaves using extraction buffer [50 mM Tris/HCl (pH 7.5), 150 mM NaCl, 1% (v/v) Triton X-100, 0.1% (w/v) SDS, phosphatase and protease inhibitors (PhosStop™ and EDTA-free Complete™, Roche)]. The SDS-PAGE separating gel consisted of 8% acrylamide, 50 μM Phos-tag acrylamide (APEXBIO, USA), 357 mM Tris buffer (pH 8.8) and 100 μM MnCl₂. Phos-tag SDS-PAGE was performed using Mn²⁺-Phos-tag SDS-PAGE according to the manufacturer's protocol.

Statistical analysis

All of the experiments in this study were performed at least three times. The error bars in each graph indicate the mean values ± standard error (SE) of replicates. Statistical significance between different measurements was assessed by Tukey's honestly significant difference (HSD) test using IBM Statistical Product and Service Solutions (SPSS) Statistics software version 19 (IBM, USA).

ACKNOWLEDGEMENTS

This work was financially supported by grants from the National Natural Science Foundation of China (Grant Nos. 31171837 and 31471424). The authors have no conflicts of interest to declare.

REFERENCES

Asai, T., Tena, G., Plotnikova, J., Willmann, M.R., Chiu, W.-L., Gomez-Gomez, L., Boller, T., Ausubel, F.M. and Sheen, J. (2002) MAP kinase signalling cascade in *Arabidopsis* innate immunity. *Nature*, **415**, 977–983.

Bekešová, S., Komis, G., Krenek, P., Vypelková, P., Ovecka, M., Luptovciak, I., Illés, P., Kucharová, A. and Šamaj, J. (2015) Monitoring protein phosphorylation by acrylamide pendant Phos-Tag™ in various plants. *Front Plant Sci.* **6**, 336.

Birkenbihl, R.P., Diezel, C. and Somssich, I.E. (2012) Arabidopsis *WRKY33* is a key transcriptional regulator of hormonal and metabolic responses toward *Botrytis cinerea* infection. *Plant Physiol.* **159**, 266–285.

Chen, X., Lu, X., Shu, N., Wang, S., Wang, J., Wang, D., Guo, L. and Ye, W. (2017) Targeted mutagenesis in cotton (*Gossypium hirsutum* L.) using the CRISPR/Cas9 system. *Sci Rep.* **7**, 44 304.

Cheong, Y.H., Moon, B.C., Kim, J.K., Kim, C.Y., Kim, M.C., Kim, I.H., Park, C.Y., Kim, J.C., Park, B.O., Koo, S.C., Yoon, H.W., Chung, W.S., Lim, C.O., Lee, S.Y. and Cho, M.J. (2003) *BWMK1*, a rice mitogen-activated protein kinase, locates in the nucleus and mediates pathogenesis-related gene expression by activation of a transcription factor. *Plant Physiol.* **132**, 1961–1972.

Delaney, T.P., Friedrich, L. and Ryals, J.A. (1995) Arabidopsis signal transduction mutant defective in chemically and biologically induced disease resistance. *Proc. Natl. Acad. Sci. USA*, **92**, 6602–6606.

Dou, L., Zhang, X., Pang, C., Song, M., Wei, H., Fan, S. and Yu, S. (2014) Genome-wide analysis of the WRKY gene family in cotton. *Mol. Genet. Genomics*, **289**, 1103–1121.

Ding, L., Xu, H., Yi, H., Yang, L., Kong, Z., Zhang, L., Xue, S., Jia, H. and Ma, Z. (2011) Resistance to hemi-biotrophic *F. graminearum* infection is associated with coordinated and ordered expression of diverse defense signaling pathways. *PLoS One*, **6**, e19008.

Feng, F. and Zhou, J.M. (2012) Plant–bacterial pathogen interactions mediated by type III effectors. *Curr. Opin. Plant Biol.* **15**, 469–476.

Frey, N.F., Garcia, A.V., Bigeard, J., Zaag, R., Bueso, E., Garmier, M., Pateyron, S., de Trazia-Moreau, M.L., Brunaud, V., Balzergue, S., Colcombet, J., Aubourg, S., Martin-Magniette, M.L. and Hirt, H. (2014) Functional analysis of *Arabidopsis* immune-related MAPKs uncovers a role for MPK3 as negative regulator of inducible defences. *Genome Biol.* **15**, R87.

Gao, M., Liu, J., Bi, D., Zhang, Z., Cheng, F., Chen, S. and Zhang, Y. (2008) MEK1, MKK1/MKK2 and MPK4 function together in a mitogen-activated protein kinase cascade to regulate innate immunity in plants. *Cell Res.* **18**, 1190–1198.

Gao, Y., Wu, Y., Du, J., Zhan, Y., Sun, D., Zhao, J., Zhang, S., Li, J. and He, K. (2017) Both light-induced SA accumulation and ETI mediators contribute to the cell death regulated by BAK1 and BKK1. *Front. Plant Sci.* **8**, 622.

Gaspar, Y.M., McKenna, J.A., McGinness, B.S., Hinch, J., Poon, S., Connelly, A.A., Anderson, M.A. and Heath, R.L. (2014) Field resistance to *Fusarium oxysporum* and *Verticillium dahliae* in transgenic cotton expressing the plant defensin NaD1. *J. Exp. Bot.* **65**, 1541–1550.

Glazebrook, J. (2005) Contrasting mechanisms of defense against biotrophic and necrotrophic pathogens. *Annu. Rev. Phytopathol.* **43**, 205–227.

Glazebrook, J., Rogers, E.E. and Ausubel, F.M. (1996) Isolation of *Arabidopsis* mutants with enhanced disease susceptibility by direct screening. *Genetics*, **143**, 973–982.

Gu, Z., Huang, C., Li, F. and Zhou, X. (2014) A versatile system for functional analysis of genes and microRNAs in cotton. *Plant Biotechnol. J.* **12**, 638–649.

He, K., Gou, X., Yuan, T., Lin, H., Asami, T., Yoshida, S., Russell, S.D. and Li, J. (2007) BAK1 and BKK1 regulate brassinosteroid-dependent growth and brassinosteroid-independent cell-death pathways. *Curr. Biol.* **17**, 1109–1115.

Ishihama, N. and Yoshioka, H. (2012) Post-translational regulation of WRKY transcription factors in plant immunity. *Curr. Opin. Plant Biol.* **15**, 431–437.

Jones, D.A. and Takemoto, D. (2004) Plant innate immunity—direct and indirect recognition of general and specific pathogen-associated molecules. *Curr. Opin. Immunol.* **16**, 48–62.

Jones, J.D. and Dangl, J.L. (2006) The plant immune system. *Nature*, **444**, 323–329.

Kishi-Kaboshi, M., Okada, K., Kurimoto, L., Murakami, S., Umezawa, T., Shibuya, N., Yamane, H., Miyao, A., Takatsuji, H., Takahashi, A. and Hirochika, H. (2010) A rice fungal MAMP-responsive MAPK cascade regulates metabolic flow to antimicrobial metabolite synthesis. *Plant J.* **63**, 599–612.

Li, Y., Zhang, L., Wang, X., Zhang, W., Hao, L., Chu, X. and Guo, X. (2013) Cotton *GhMPK6a* negatively regulates osmotic tolerance and bacterial infection in transgenic *Nicotiana benthamiana*, and plays a pivotal role in development. *FEBS J.* **280**, 5128–5144.

Li, Y., Zhang, L., Lu, W., Wang, X., Wu, C.A. and Guo, X. (2014) Overexpression of cotton GhMCK4 enhances disease susceptibility and affects abscisic acid, gibberellin and hydrogen peroxide signalling in transgenic *Nicotiana benthamiana*. *Mol. Plant Pathol.* **15**, 94–108.

Longoni, P., Douchi, D., Cariti, F., Fucile, G. and Goldschmidt-Clermont, M. (2015) Phosphorylation of the light-harvesting complex II isoform Lhcb2 is central to state transitions. *Plant Physiol.* **169**, 2874–2883.

- MAPK Group. (2002) Mitogen-activated protein kinase cascades in plants: a new nomenclature. *Trends Plant Sci.* **7**, 301–308.
- Medzhitov, R. and Janeway, C.A. Jr. (1997) Innate immunity: the virtues of a non-clonal system of recognition. *Cell*, **91**, 295–298.
- Meng, X. and Zhang, S. (2013) MAPK cascades in plant disease resistance signaling. *Annu. Rev. Phytopathol.* **51**, 245–266.
- Morrissey, J.P. and Osbourn, A.E. (1999) Fungal resistance to plant antibiotics as a mechanism of pathogenesis. *Microbiol. Mol. Biol. Rev.* **63**, 708–724.
- Ospina-Giraldo, M.D., Mullins, E. and Kang, S. (2003) Loss of function of the *Fusarium oxysporum* SNF1 gene reduces virulence on cabbage and *Arabidopsis*. *Curr. Genet.* **44**, 49–57.
- Pan, J., Zhang, M., Kong, X., Xing, X., Liu, Y., Zhou, Y., Liu, Y., Sun, L. and Li, D. (2012) *ZmMPK17*, a novel maize group D MAP kinase gene, is involved in multiple stress responses. *Planta*, **235**, 661–676.
- Page, J.T., Huynh, M.D., Liechty, Z.S., Grupp, K., Stelly, D., Hulse, A.M., Ashrafi, H., Van Deynze, A., Wendel, J.F. and Udall, J.A. (2013) Insights into the evolution of cotton diploids and polyploids from whole-genome re-sequencing. *G3 (Bethesda)*, **3**, 1809–1818.
- Pedley, K.F. and Martin, G.B. (2004) Identification of MAPKs and their possible MAPK kinase activators involved in the *Pto*-mediated defense response of tomato. *J. Biol. Chem.* **279**, 49 229–49 235.
- Peng, X., Hu, Y., Tang, X., Zhou, P., Deng, X., Wang, H. and Guo, Z. (2012) Constitutive expression of rice *WRKY30* gene increases the endogenous jasmonic acid accumulation, PR gene expression and resistance to fungal pathogens in rice. *Planta*, **236**, 1485–1498.
- Pietro, A.D., Madrid, M.P., Caracuel, Z., Delgado-Jarana, J. and Roncero, M.I. (2003) *Fusarium oxysporum*: exploring the molecular arsenal of a vascular wilt fungus. *Mol. Plant Pathol.* **4**, 315–325.
- Rep, M., Meijer, M., Houterman, P.M., van der Does, H.C. and Cornelissen, B.J. (2005) *Fusarium oxysporum* evades I-3-mediated resistance without altering the matching avirulence gene. *Mol. Plant-Microbe Interact.* **18**, 15–23.
- Rodríguez, M.C., Petersen, M. and Mundy, J. (2010) Mitogen-activated protein kinase signaling in plants. *Annu. Rev. Plant Biol.* **61**, 621–649.
- Rogers, E. and Ausubel, F.M. (1997) *Arabidopsis* enhanced disease susceptibility mutants exhibit enhanced susceptibility to several bacterial pathogens and alterations in *PR-1* gene expression. *Plant Cell*, **9**, 305–316.
- Rushton, P.J., Somssich, I.E., Ringler, P. and Shen, Q.J. (2010) WRKY transcription factors. *Trends Plant Sci.* **15**, 247–258.
- Schechter, L.M., Vencato, M., Jordan, K.L., Schneider, S.E., Schneider, D.J. and Collmer, A. (2006) Multiple approaches to a complete inventory of *Pseudomonas syringae* pv. *tomato* DC3000 type III secretion system effector proteins. *Mol. Plant-Microbe Interact.* **19**, 1180–1192.
- Shi, J., An, H.L., Zhang, L., Gao, Z. and Guo, X. (2010) *GhMPK7*, a novel multiple stress-responsive cotton group C MAPK gene, has a role in broad spectrum disease resistance and plant development. *Plant Mol. Biol.* **74**, 1–17.
- Shi, J., Zhang, L., An, H., Wu, C. and Guo, X. (2011) *GhMPK16*, a novel stress-responsive group D MAPK gene from cotton, is involved in disease resistance and drought sensitivity. *BMC Mol. Biol.* **12**, 22.
- Sunilkumar, G., Campbell, L.M., Puckhaber, L., Stipanovic, R.D. and Rathore, K.S. (2006) Engineering cottonseed for use in human nutrition by tissue-specific reduction of toxic gossypol. *Proc. Natl. Acad. Sci. USA*, **103**, 18 054–18 059.
- Thaler, J.S., Humphrey, P.T. and Whiteman, N.K. (2012) Evolution of jasmonate and salicylate signal crosstalk. *Trends Plant Sci.* **17**, 260–270.
- Vlot, A.C., Dempsey, D.A. and Klessig, D.F. (2009) Salicylic acid, a multifaceted hormone to combat disease. *Annu. Rev. Phytopathol.* **47**, 177–206.
- Walia, A., Lee, J.S., Wasteneys, G. and Ellis, B. (2009) *Arabidopsis* mitogen-activated protein kinase *MPK18* mediates cortical microtubule functions in plant cells. *Plant J.* **59**, 565–575.
- Wang, C., Ulloa, M. and Roberts, P.A. (2006) Identification and mapping of micro-satellite markers linked to a root-knot nematode resistance gene (*RKN1*) in Acala NemX cotton (*Gossypium hirsutum* L.). *Theor. Appl. Genet.* **112**, 770–777.
- Wang, C., Lu, W., He, X., Wang, F., Zhou, Y., Guo, X. and Guo, X. (2016) The cotton mitogen-activated protein kinase 3 functions in drought tolerance by regulating stomatal responses and root growth. *Plant Cell Physiol.* **57**, 1629–1642.
- Wang, F., Wang, C., Yan, Y., Jia, H. and Guo, X. (2016) Overexpression of cotton *GhMPK11* decreases disease resistance through the gibberellin signaling pathway in transgenic *Nicotiana benthamiana*. *Front Plant Sci.* **7**, 689.
- Wang, X., Xiao, H., Chen, G., Zhao, X., Huang, C., Chen, C. and Wang, F. (2011) Isolation of high-quality RNA from *Reaumuria soongorica*, a desert plant rich in secondary metabolites. *Mol. Biotechnol.* **48**, 165–172.
- Wang, X., Yan, Y., Li, Y., Chu, X., Wu, C. and Guo, X. (2014) *GhWRKY40*, a multiple stress-responsive cotton WRKY gene, plays an important role in the wounding response and enhances susceptibility to *Ralstonia solanacearum* infection in transgenic *Nicotiana benthamiana*. *PLoS One*, **9**, e93577.
- Wang, X.J., Zhu, S.-Y., Lu, Y.F., Zhao, R., Xin, Q., Wang, X.F. and Zhang, D.P. (2010) Two coupled components of the mitogen-activated protein kinase cascade MdMPK1 and MdMKK1 from apple function in ABA signal transduction. *Plant Cell Physiol.* **51**, 754–766.
- Yan, Y., Jia, H., Wang, F., Wang, C., Liu, S. and Guo, X. (2015) Overexpression of *GhWRKY27a* reduces tolerance to drought stress and resistance to *Rhizoctonia solani* infection in transgenic *Nicotiana benthamiana*. *Front Physiol.* **6**, 265.
- Yang, B., Wang, Q., Jing, M., Guo, B., Wu, J., Wang, H., Wang, Y., Lin, L., Wang, Y., Ye, W., Dong, S. and Wang, Y. (2017) Distinct regions of the *Phytophthora* essential effector Avh238 determine its function in cell death activation and plant immunity suppression. *New Phytol.* **214**, 361–375.
- Yang, K.Y., Liu, Y. and Zhang, S. (2001) Activation of a mitogen-activated protein kinase pathway is involved in disease resistance in tobacco. *Proc. Natl. Acad. Sci. USA*, **98**, 741–746.
- Yoo, S.D., Cho, Y.H. and Sheen, J. (2007) *Arabidopsis* mesophyll protoplasts: a versatile cell system for transient gene expression analysis. *Nat. Protoc.* **2**, 1565–1572.
- Yu, F., Huaxia, Y., Lu, W., Wu, C., Cao, X. and Guo, X. (2012) *GhWRKY15*, a member of the WRKY transcription factor family identified from cotton (*Gossypium hirsutum* L.), is involved in disease resistance and plant development. *BMC Plant Biol.* **12**, 144.
- Yu, X., Tang, J., Wang, Q., Ye, W., Tao, K., Duan, S., Lu, C., Yang, X., Dong, S., Zheng, X. and Wang, Y. (2012) The RxLR effector Avh241 from *Phytophthora sojae* requires plasma membrane localization to induce plant cell death. *New Phytol.* **196**, 247–260.
- Zhang, J., Shao, F., Li, Y., Cui, H., Chen, L., Li, H., Zou, Y., Long, C., Lan, L., Chai, J., Chen, S., Tang, X. and Zhou, J.M. (2007) A *Pseudomonas syringae* effector inactivates MAPKs to suppress PAMP-induced immunity in plants. *Cell Host Microbe*, **1**, 175–185.
- Zhang, L., Xi, D., Luo, L., Meng, F., Li, Y., Wu, C.A. and Guo, X. (2011) Cotton *GhMPK2* is involved in multiple signaling pathways and mediates defense responses to pathogen infection and oxidative stress. *FEBS J.* **278**, 1367–1378.
- Zhang, L., Li, Y., Lu, W., Meng, F., Wu, C.A. and Guo, X. (2012) Cotton *GhMKK5* affects disease resistance, induces HR-like cell death, and reduces the tolerance to salt and drought stress in transgenic *Nicotiana benthamiana*. *J. Exp. Bot.* **63**, 3935–3951.
- Zhang, T., Chen, S. and Harmon, A.C. (2016) Protein–protein interactions in plant mitogen-activated protein kinase cascades. *J. Exp. Bot.* **67**, 607–618.
- Zhang, X., Xu, X., Yu, Y., Chen, C., Wang, J., Cai, C. and Guo, W. (2016) Integration analysis of MKK and MAPK family members highlights potential MAPK signaling modules in cotton. *Sci Rep.* **6**, 29 781.

SUPPORTING INFORMATION

Additional Supporting Information may be found in the online version of this article at the publisher's website:

Fig. S1 Mitogen-activated protein kinase (MAPK) expression patterns were analysed after cotton seedlings were infected with *Fusarium oxysporum*. (A) Expression pattern of *GhMPK20* in cotyledon after *F. oxysporum* infection. (B) Expression pattern of *GhMPK20* after root wounding. (C) Expression pattern of *GhMPK6* after *F. oxysporum* infection. (D) Expression pattern of *GhMPK7* after *F. oxysporum* infection. (E) Expression pattern of *GhMPK11* after *F. oxysporum* infection. (F) Expression pattern of *GhMPK16* after *F. oxysporum* infection. Data are presented as the mean \pm standard error (SE) of three independent experiments ($n = 6$). The letters above the columns represent significant differences ($P < 0.05$) based on Tukey's honestly significant difference (HSD) test.

Fig. S2 Phylogenetic analysis of GhMPK20 and other plant mitogen-activated protein kinase (MAPK) proteins. The neighbour-joining phylogenetic tree was constructed using MEGA 4.0. The numbers above or below the branches indicate the bootstrap values (>50%) from 500 replicates. The GenBank IDs follow the protein names. The abbreviations of the species names are as follows: At, *Arabidopsis thaliana*; Gh, *Gossypium hirsutum*; Nt, *Nicotiana tabacum*; Zm, *Zea mays*; Le, *Lycopersicon esculentum*; Mt, *Medicago truncatula*.

Fig. S3 Sodium dodecylsulfate-polyacrylamide gel electrophoresis (SDS-PAGE) of transiently expressed proteins (35S::GFP and 35S::GhMPK20-GFP) followed by western blotting with anti-green fluorescent protein (anti-GFP). 1, *Nicotiana benthamiana* leaves transiently expressing the 35S::GFP plasmid using *Agrobacterium* infiltration; 2, *N. benthamiana* leaves transiently expressing the 35S::GhMPK20-GFP plasmid using *Agrobacterium* infiltration.

Fig. S4 GhMPK20 expression levels in nine independent transgenic lines obtained from T1 progeny. WT, wild-type.

Fig. S5 GhMCK4 expression levels in GhMCK4-silenced cotton plants. The error bars indicate the mean \pm standard error (SE) of three independent experiments ($n = 6$). The letters above the columns represent significant differences ($P < 0.05$) based on Tukey's honestly significant difference (HSD) test.

Fig. S6 Phosphorylation assay using Phos-tag polyacrylamide gel electrophoresis (PAGE). (A) Phosphorylation assay of GhMPK20 in cotton protoplasts transformed with GhMPK20-MYC or co-transformed with GhMCK4-FLAG and GhMPK20-MYC by western blotting. (B) Phosphorylation assay of

GhWRKY40 in cotton protoplasts transformed with GhWRKY40-FLAG or co-transformed with GhMPK20-MYC and GhWRKY40-FLAG by western blotting. P and U indicate the phosphorylated and unphosphorylated forms, respectively.

Fig. S7 GhWRKY40 expression levels were analysed after cotton seedlings were infected with *Fusarium oxysporum*. Data are presented as the mean \pm standard error (SE) of three independent experiments ($n = 6$). The letters above the columns represent significant differences ($P < 0.05$) based on Tukey's honestly significant difference (HSD) test.

Fig. S8 Expression levels of *PDF1.2* and salicylic acid (SA)-mediated defence pathway genes in GhWRKY40-silenced cotton after *Fusarium oxysporum* infection. The error bars indicate the mean \pm standard error (SE) of three independent experiments ($n = 6$). The letters above the columns represent significant differences ($P < 0.05$) based on Tukey's honestly significant difference (HSD) test.

Fig. S9 Expression levels of salicylic acid (SA)- and jasmonic acid (JA)-mediated defence pathway genes in wild-type cotton before infection or after *Fusarium oxysporum* infection for 5 days. The error bars indicate the mean \pm standard error (SE) of three independent experiments ($n = 6$). The letters above the columns represent significant differences ($P < 0.05$) based on Tukey's honestly significant difference (HSD) test.

Fig. S10 Representative phenotypes of GhWRKY40-silenced cotton after infection with *Fusarium oxysporum* for 5 days by the external application of salicylic acid (SA) (10 mM).

Table S1 Primers used in this study.